Ibn Al-Haitham Journal for Pure and Applied Sciences
Journal homepage: jih.uobaghdad.edu.iq
PISSN: 1609-4042, EISSN: 2521-3407
IHJPAS. 2026; 39(1)

Comparative Histopathological Study of Ciprofloxacin Impact on *Mus musculus* Renal Cortex Infected with Multi-drug Resistance and Susceptible Uropathogenic *Escherichia Coli*

Omar Sinan Sadiq Hussain Al-Zaidi[1,2*], Estabraq A. Mahmoud[1] and Luma Abdulhady Zwain[1]

Department of Biology, College of Education for Pure Sciences (Ibn Al-Haitham),University of Baghdad,Baghdad,Iraq
[2]National Center of Hematology, Mustansiriyah University, Baghdad, Iraq
*Corresponding Author

Received: 22/May/2025
Accepted:30/September/2025
Published: 20/January/2026
doi.org/10.30526/39.1.4204

Abstract

Urinary tract infections are mainly caused by uropathogenic *Escherichia coli*, which represent a significant global issue along with the rising of antibiotic resistance and treatment challenges. The aim of this study was to evaluate ciprofloxacin efficacy as a treatment in animal models following infection with multidrug-resistant UPEC and multidrug-susceptible UPEC and to determine the nephrotoxic effect of these antibiotics on the renal cortex. Up to 76 *E. coli* isolates were collected from UTI patients in Baghdad province, characterized by morphological and biochemical features, and confirmed using the Vitek-2 compact system. Mice were orally infected via gastric gavage with G33 using a bacterial load of 107 cells/ml, followed by post-infection treatment strategies with the aid of ciprofloxacin post-infection. Efficacy was determined by reduction in bacterial load, body weight, and renal cortex cross-sections. Ciprofloxacin significantly reduced the bacterial load but also caused toxicity to the kidney, such as tubular necrosis, hemorrhage, and congestion of glomeruli. This study highlights the urgent need for specialized antibiotic treatment systems to reduce drug resistance and nephrotoxicity effects. Further studies are essential to minimize renal damage.

Keywords: UPEC, Ciprofloxacin, Renal cortex, renal medulla Antibiotic resistance.

1. Introduction

Urinary tract infections (UTIs) are considered one of the most common bacterial infectious diseases worldwide, affecting well over 150 million people each year[1]. *Escherichia coli*, a member of the Enterobacteriaceae family, is considered the predominant pathogen of urinary tract infections worldwide and is also responsible for many other cases such as wound infections, otitis media, and meningitis [3, 4]. Nearly 80% of clinical cases related to UTIs are caused by UPEC and these cases are highly incident in women[1]. *E. coli* possess many virulence factors such as toxins, adhesion factors and biofilm, which provides a barrier to limit the penetration of antibiotics[5] and is considered a major concern for public health and thus leads to treatment strategies and leads to high morbidity and costly healthcare [6]. Empirical therapy with antibiotics is the cornerstone for UTIs; antibiotics such as ciprofloxacin, trimethoprim/sulfamethoxazole, nitrofurantoin, fosfomycin, and ceftriaxone are described as agents for UTI treatment. However, resistance to fluoroquinolones arises in *E. coli* and becomes a major concern. Similarly,

trimethoprim/sulfamethoxazole, which is described as a UTI treatment, has high resistance rates globally recorded for its limited effectiveness [7, 8]. Along with the antibiotic resistance challenges, the nephrotoxic effect of these antibiotics should be monitored. Such antibiotics, known for their nephrotoxic effects, significantly cause kidney injuries, especially in hospitalized patients, and thus lead to increased mortalities [9]. The mechanism of renal toxicity includes damage to renal tubule cells and alteration in the renal hemodynamics. Ciprofloxacin indicates nephrotoxicity activity, especially at high doses [10, 11]. There is an urgent need to evaluate the efficacy and safety of these antibiotics, which are used as treatment for UTIs. Animal models, such as mice, provide valuable results of physiological and histopathological alterations during UTI. Thus, the present study aimed to investigate ciprofloxacin effectiveness in treating UTIs caused by multi-drug-resistant UPEC and multi-drug-susceptible UPEC in animal models. By determination of bacterial load reduction, renal cortex histopathological changes, and some side effects of these antibiotics on body weight and mortality rates.

2. Materials and Methods

2.1 Bacterial isolates sampling and antibiotics

Seventy-six isolates, as listed in **Table 1**, belonging to the genus *Escherichia*, were collected from the urine of UTI patients from various hospitals in Baghdad province for the period December 2023 to February of 2024 after the ethical approval for sampling from the Iraqi Ministry of Health's ethical review board. Isolates collected from different genders and ages ranged from 15 days to 84 years, followed by characterization of them by using morphological and biochemical identification, which includes oxidase, catalase, indole, methyl red, and Voges-Proskauer [12].

Table 1. Numbers and percentages of bacterial isolates.

Institution	Number of Bacterial isolates
Kadhimiya Educational Hospital	56 (73.6)%
Ghazi Al-Hariri Hospital for Surgical Specialties	19 (25)%
Imam Ali Hospital	1 (1.4)%

After the primary identification, the Vitek®-2 compact system (BioMérieux, France) was used to confirm the identification by using GNID cards provided by BioMérieux, France, followed by Antimicrobial Sensitivity Tests (AST) using AST cards provided by BioMérieux, France. Ciprofloxacin was used for the treatment of infected animals in this study. Ciprofloxacin powder was provided by Al-Jazeera for the pharmaceutical company. Ciprofloxacin was prepared as suspensions in sterilized distilled water at concentrations of 500 mg/kg and then adjusted to suit the treatment of infected mice with recommended dosages outlined in [13].

2.2 Experimental Animals

Sixty-six Female mice aged 8-10 weeks were bought from the animal house of the Iraqi Center for Cancer Research and Medical Genetics, Al-Mustansiriya University, Iraq. The animals were housed in a controlled environment at an appropriate temperature of 27ºC. Animals were provided with chow and water. The animals acclimatized for five days before the experiment to minimize stress and ensure adaptation to the environment. The mice were randomly assigned into seven groups based on body weight. Each group was housed in individual cages equipped with metal mesh lids to ensure monitoring, security, and prevention of escape of animals.

2.3 Pilot Study

A pilot study was conducted to determine the most effective method and bacterial load required to induce urinary tract infections (UTIs) in female mice using uropathogenic *E. coli* (UPEC). Two methods evaluated oral administration and intraperitoneal injection. The selected isolates were G33 and G27. The G33 isolate was resistant to multiple antibiotics (amoxicillin, ampicillin,

amoxicillin/clavulanic acid, ticarcillin, piperacillin, piperacillin/tazobactam, cefazolin, cefuroxime, cefoxitin, cefixime, ceftazidime, ceftizoxime, ceftrixone, cefepime, ertapenem, imipenem, meropenem, amikacin, gentamicin, ciprofloxacin, levofloxacin, tigecycline, nitrofurantoin, and trimethoprim/sulfamethoxazole), while G27 was susceptible to the same antibiotics. The selected isolates were suspended in 1ml normal saline, and serial dilutions of 105, 106, 107, and 109 cells/ml were made to evaluate their ability to induce UTIs. Infectivity was assessed 24 and 48 hours post administration. Mice were euthanized, and kidneys were aseptically removed for analysis. Each kidney was carefully homogenized in 1 ml of normal saline, and serial dilutions were made to be cultured. Subsequently, 100 µl of each dilution was cultured on MacConkey agar using a sterile glass rod, and the plates were incubated for 24 h at 37°C to determine the bacterial colony count.

2.4 Murine induction and antibiotic administration

To evaluate the effect of ciprofloxacin as a treatment on the bacterial load of female murine modules induced by both G33 and G27. Groups divided to study various conditions of kidney tissue in murine modules. According to the pilot study, the oral route was found to successfully establish UTI in murine models, so the oral route was chosen for the experimental design. The experimental animals were divided into 7 groups, each group comprising three animals for the multi-drug resistance isolate (G33) experiment and five animals for the multi-drug Susceptible as follows: Group 1 orally administered distilled water only (control). Group 2 was administered ciprofloxacin 500 mg/kg twice daily 48 hours after the experiment commenced for five days. Group 3 was administered ciprofloxacin at a concentration of 500 mg/kg twice daily 72 hours after the experiment commenced for five days. The selected isolates G33 and G27 were used to induce UTIs by oral administration of 107 cells/ml for two days in groups 4 and 6 and for three days in groups 5 and 7. Following this, groups 6 and 7 were treated with Ciprofloxacin 500mg/kg for 5 days (twice daily). Group 1 represented the control, and groups 2 and 3 represented the negative control. Groups 4 and 5 represented the positive control, while the rest of the groups represented the test groups, as shown in **Table 2**.

Table 2. Experimental Group Design and Treatment Schedule

Mice group	Administration	Days	Treatment	Status
1	Distal Water	5-7	-	Control
2	Ciprofloxacin 500 mg/kg	5	-	Negative Control (2 days)
3	Ciprofloxacin 500 mg/kg	5	-	Negative Control (3days)
4	G33/G27 (10^7cell/ml)	2	-	Positive Control
5	G33/G27 (10^7cell/ml)	3	-	Positive Control
6	G33/G27 (10^7cell/ml)	2	CIP	Test group
7	G33/G27 (10^7cell/ml)	3	CIP	Test group

2.5 Histopathological study

Kidney tissues were collected from all groups of mice for histopathological examination. After gross observations, the kidneys were fixed in 10% buffered formalin until histopathological sections were made. The kidneys are treated with alcohol, xylene, and paraffin to remove impurities and then embedded in paraffin wax. The kidneys are then cut at 4-µm thickness and mounted on slides for Hematoxylin and Eosin (H&E) to examine [14].

3. Results

3.1 Bacterial isolates identification

All 76 isolates produced dry, pink, lactose-fermenting colonies on MacConkey agar. Biochemical tests showed negative oxidase and catalase, positive indole (except 4 variable), positive methyl red, and negative Voges–Proskauer and citrate, consistent with *E.coli*. The Vitek®-2 compact system confirmed 70/76 isolates (93–99% confidence); 49 (70%) were from females and 21 (30%) from males.

3.2 Pilot study

According to the pilot study results, the results revealed that the bacterial loads of 105 and 106 cells/ml were insufficient to induce UTIs in mice whether the infection was introduced orally or via the intraperitoneal injection route. No colonies (0 CFU/mL) were detected after 24 and 48 hours post-infection, which means an absence of infection in the urinary system. These findings suggest that the lower bacterial concentrations of E. coli were unable to overcome host immune defenses. The lack of bacterial colonization was determined in two ways: the first one was gross observation of the kidney, which seemed just like the normal kidney in morphology and weight. The second way is determined by no formation of bacterial colonies after performing a serial dilution for the kidney. Otherwise, the bacterial load of 107 cells/ml was found to be effective in inducing infection in the kidney after oral administration. This evidence was demonstrated after observing bacterial growth 24 hours post-infection.

3.3 Body Weight and Mortality-MDR UPEC (G33)

At the beginning of the experiment, all animals were weighed, and the weight was recorded at two-day intervals across the experiment. Groups 2 and 3, which were administered ciprofloxacin, showed gradual decreases in weight. In groups 4 and 5, a significant increase in weight was observed; especially group 5 showed higher weight gain compared to group 4. In the test groups, groups 6 and 7, which were treated with ciprofloxacin, group 6 displayed a gradual increase in weight, while group 7 displayed a consistent decrease in weight. These results highlight the impact of antibiotics and infection on weight change across the study compared to the control group, which displayed a consistent increase in weight over the study as shown in **Figure 1.**

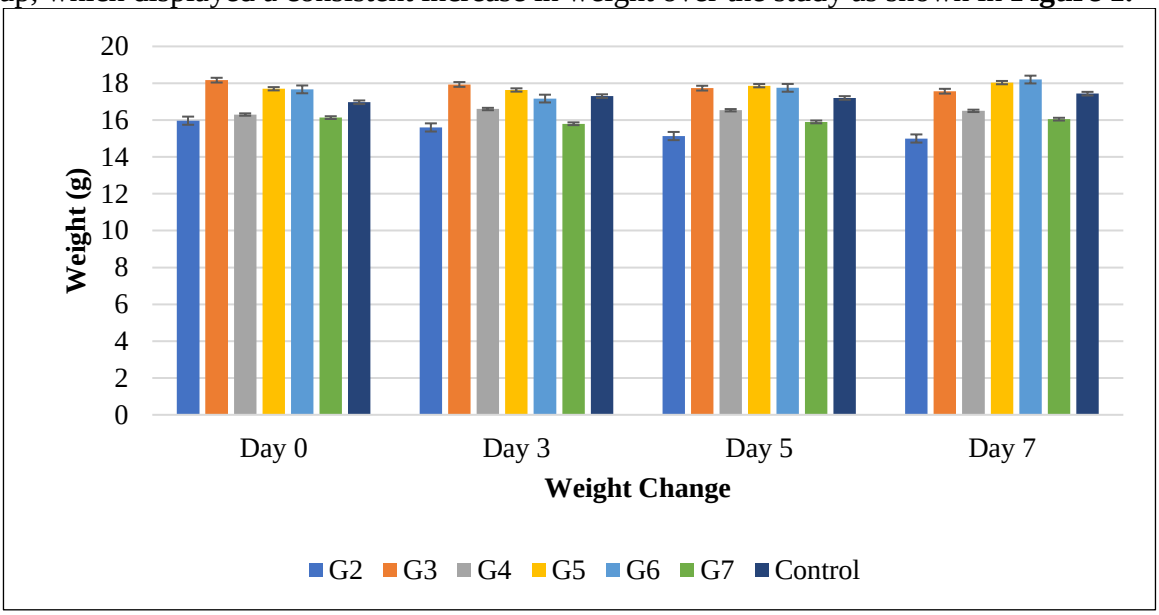

Figure 1. Body weight change of animals cross the experiment with MDR-UPEC (G33), *Group 2 (G2), Group 3 (G3), Group 4 (G4), Group 5 (G5), Group 6 (G6) & Group 7 (G7).

The dose of 10^7 cells/mL was identified as optimal for establishing infection without causing mortality. In contrast, intraperitoneal injection of 107 cells/ml was insufficient to induce kidney infection, as no bacterial colonies were detected on MacConkey agar. Furthermore, administration of 109 cells/ml, no matter the route, resulted in immediate mortality of animals. The results revealed differences in mortality, behavior, and weight changes among the experimental groups. In the negative control groups, lethargy was observed within groups 2 and 3. The mortality rate reached 2 (66.6%) within group 2 animals; one animal died after the second dose of ciprofloxacin, and another one died an hour and a half after dosing with the first half of the fourth dose of ciprofloxacin. As for group 3, no mortalities were recorded. The positive control groups 4 and 5, which were infected with the selected isolate (G33), scored 0% mortality and hyperactivity within animals after administration of the bacterial dose. Test groups 6 and 7,

treated with ciprofloxacin, display hyperactivity initially but transition to lethargy. One animal (33.3%) of group 6 died immediately after the first half of the second dose, while the rest of the animals in the group did not die. As for group 7, the mortality rate reached 2 (66.6%). One animal died after the first half of the second dose, and another one died after being dosed with the second half of the third dose, while the control group showed normal behavior with no mortalities, as shown in **Figure 2**.

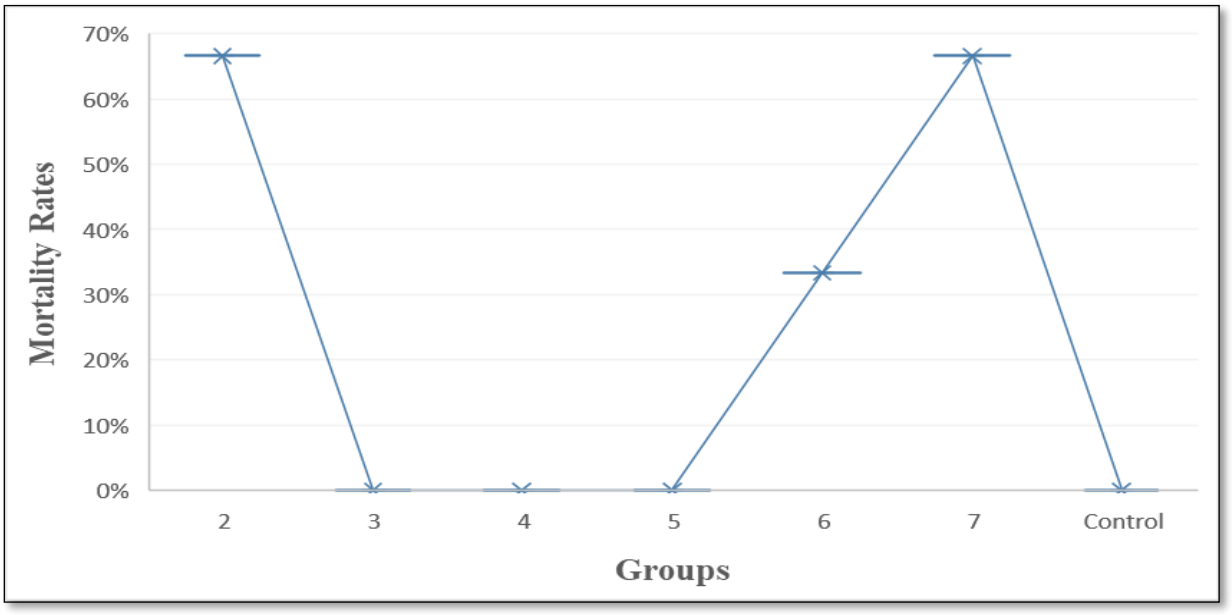

Figure 2. The mortality rates across the experiment with MDR-UPEC.

3.4 Weight change, multi-drug susceptible isolate (G27) administration and treatment

At the beginning of the experiment, all animals were weighed, and the weight was recorded at two-day intervals across the experiment. Group 2 exhibited modest weight gain, while group 3 showed a stable increase in weight. As for groups 4 and 5, all scored slight weight variations with insignificant changes and maintained stability. Groups 6 and 7 achieved the highest weights. While the control group (group 1) shows a gradual weight gain. These results highlight the impact of antibiotics and infection on weight change across the study compared to the control group, which displayed a gradual increase in weight over the study as shown in **Figure 3**.

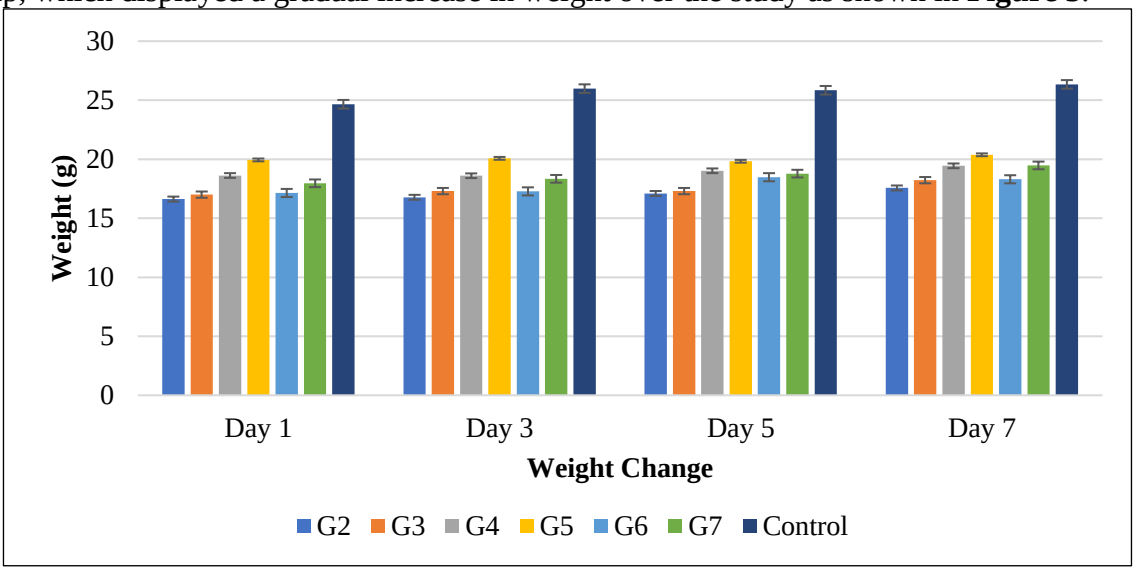

Figure 3. Body weight change of animals cross the experiment with MDS-UPEC (G27) *Group 2 (G2), Group 3 (G3), Group 4 (G4), Group 5 (G5), Group 6 (G6) & Group 7 (G7).

Differences in mortality, behavior and weight changes among the groups noted. In the negative control groups, little lethargy noticed within group 2 and 3. The mortality rates reached 2(40%) within group 2 animals, one animal 20% die after the first half of the first dose of ciprofloxacin and another one 20% after the first half of the second dose. As for group 3, also one animal (20%) died after receiving the first half of the fifth dose of ciprofloxacin. The positive control groups 4 and 5, which were infected with the selected isolate (G27), scored 1 (20%) mortality and hyperactivity within group 5 animals after administration of the bacterial dose.

The 6 and 7 groups showed hyperactivity similar to the 4 and 5 groups after being inducted with G27 at a bacterial load of 107 cells/ml. When the 6 and 7 groups were treated with ciprofloxacin and after 24 hours of induction, it was noted that the animals' activity gradually began to become lethargic; one animal (20%) scored mortality for group 6 after the first half of the second dose, while the rest of the animals in the group did not die. One animal (20%) of group 7 died immediately after receiving the first half of the fifth dose, while other animals of the group stayed alive. All animals were weighed at the beginning of the experiment at a weight/two-day rate, as it was noted that the average weights of the animals were constantly increasing during the experiment period, as shown in **Figure 4**.

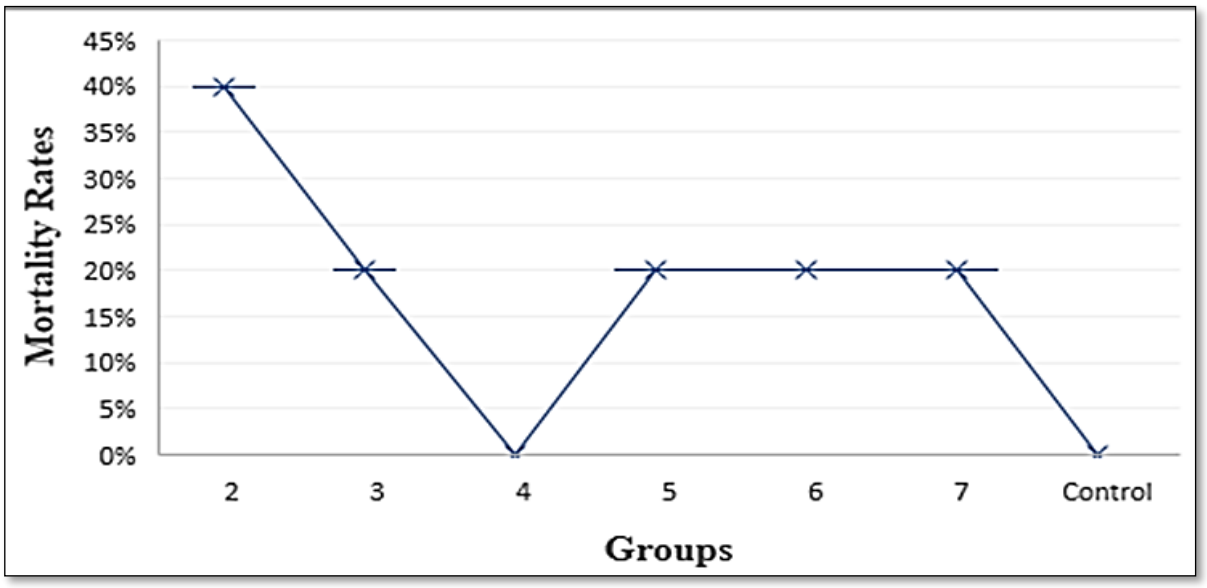

Figure 4. The mortality rates across the experiment with MDS-UPEC (G27).

3.5 Histopathological cross sections of MDR-UPEC

According to the results of the histopathological study, cross-sections as shown in **Figures 5A** and **5B** revealed normal renal cortex of the control group after staining with Hematoxylin and Eosin (H&E). The normal mouse kidney is composed of tubular epithelial cells, distal and proximal convoluted tubules, podocytes, endothelial cells, mesangial cells, Bowman's capsule, and capsular space. **Figures 5A** and **5B** represent the normal histological structure of kidney tissue. Normal proximal and distal convoluted tubules with limning epithelial cells with no signs of necrosis, cellular debris, or vacuolar degeneration within the lumen. The glomeruli appear uniform in structure and surrounded by Bowman's capsule with no signs of congestion, atrophy, or any damage of podocytes. No signs of hemorrhage and normal blood vessels.

Figures 5C and **5D** illustrate the cross-sections of the group 2 renal cortex, in which the group orally received ciprofloxacin for 5 days after 48 hours of the experiment. Early signs of kidney injury are revealed in these sections, represented by the nephrotoxic effects of ciprofloxacin. Intracellular gaps were noticed within the lining cells of convoluted tubules (proximal and distal), which refer to vascular degeneration. The degeneration represents a sign of cellular damage resulting from oxidative stress or disruption in the metabolic process by ciprofloxacin.

In addition, within glomeruli, mild atrophy was evident and changes in the podocytes. In addition, cellular debris observed within lumens of renal tubules indicates early-stage tubular epithelial cell necrosis. No signs of hemorrhage. These observations emphasize ciprofloxacin nephrotoxic effect, especially at high or prolonged doses. Also, these findings underscore the importance of continuously monitoring kidney functions to limit adverse effects of ciprofloxacin on renal health. Cross sections presented in **Figures (5E, 5F & 5G)** of group 3 after oral administration of ciprofloxacin for 5 days after 72 hours of the experiment revealed significant progression of kidney damage compared to group 2 and the control group. These sections also revealedmoderate to severe vacuolar degeneration of the tubular lining cells of proximal and distal convoluted tubules. Tubular necrosis was observed, which is indicated by the necrosis of the lining cells of the urinary tubules and glomerular cells. In addition, tubular casts (necrotic debris) within the lumen and hemorrhage were observed.

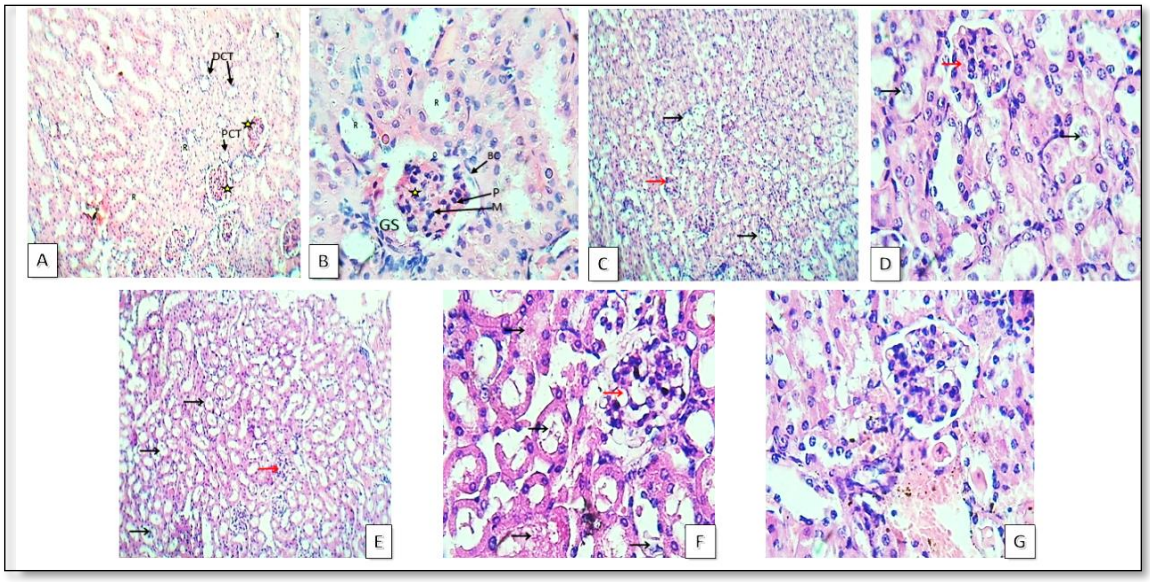

Figure 5. A-G, Cross Section of renal cortex and medulla in Mouse female (*Mus musculus*) stained with H&E. 5A&5B-sections, shows renal glomeruli (Asterisks), Renal tubule (R), Proximal Convoluted Tubule (PCT), Distal Convoluted Tubule (DCT), Glomeruli Space (GS), Mesangial cells (M), Podocytes (P) and Bowman's Capsule (BC). 5C&5D-sections shows mild degeneration of tubular epithelial cells with minimum glomeruli atrophy (Red arrow). E-G sections showing sever vacuolar degeneration (black arrows) with necrosis of Podocytes (Red arrow). Cross sections (A, C and E) (H&E, 10X). Cross-Sections (B, D, F & G) (H&E, 40x).

Sections from **Figures 6A** and **6B** of group 4 illustrate the severity of renal cortex damage after oral administration of the multi-drug resistance isolate (G33) without treatment and the impact of bacterial infection on renal tissue. Notable and widespread necrosis of renal lining epithelial cells was observed, and marked congestion of the glomeruli led to a reduction in the interstitial space of Bowman's capsule. There were no visible signs of bleeding.

As for group 5, the histological sections in Figures 6C and 6D showed extensive damage to the kidney compared to group 4. The lining cells of renal tubules showed extensive degeneration and necrosis with glomeruli atrophy, indicating that prolonged exposure to the bacteria leads to more toxic effects compared to short exposure. As distinguished, the interstitial space is affected by the presence of hemorrhage, which is represented by the clear presence of red blood cells, indicating weakness and rupture of the blood vessels. These hemorrhagic changes indicate severe vascular weakness, including rupture of the smallest capillaries and increased vascular permeability. These findings in **Figures 6A, 6B, 6C, and 6D** determine the impact of bacterial infection of UPEC on renal health. The histological sections of group 6 in **Figures 6E** and **6F** showed slight minor degeneration of lining cells of renal tubules with minor congestion of the glomeruli and clarity of Bowman's capsule after treatment with ciprofloxacin for a 5-day period.

No significant necrosis or hemorrhage observed within the interstitial space. The glomeruli was slightly congested, but the Bowman's capsule stayed integrated. These findings indicate the therapeutic effect of ciprofloxacin on the bacterial infection, despite the selected isolate being resistant, but still ciprofloxacin reduced the bacterial load. The results also indicate the effectiveness of ciprofloxacin when the duration of exposure to the bacterial infection is short.

Group 7 histological sections presented in **Figures 6G** and **6H** showed signs of kidney disease as a result of the prolonged cumulative effect of the bacterial infection. The sections showed the appearance of degeneration of lining epithelial cells of renal tubules with the appearance of severe necrosis and congestion of the glomerulus, in addition to noting podocyte degeneration and hemorrhage within the interstitial space, which indicates the destruction of blood vessels. These observations indicate that prolonged exposure to bacterial infection and delayed therapeutic strategies reduce the effectiveness of treatment with the ciprofloxacin, resulting in severe damage to renal tissue.

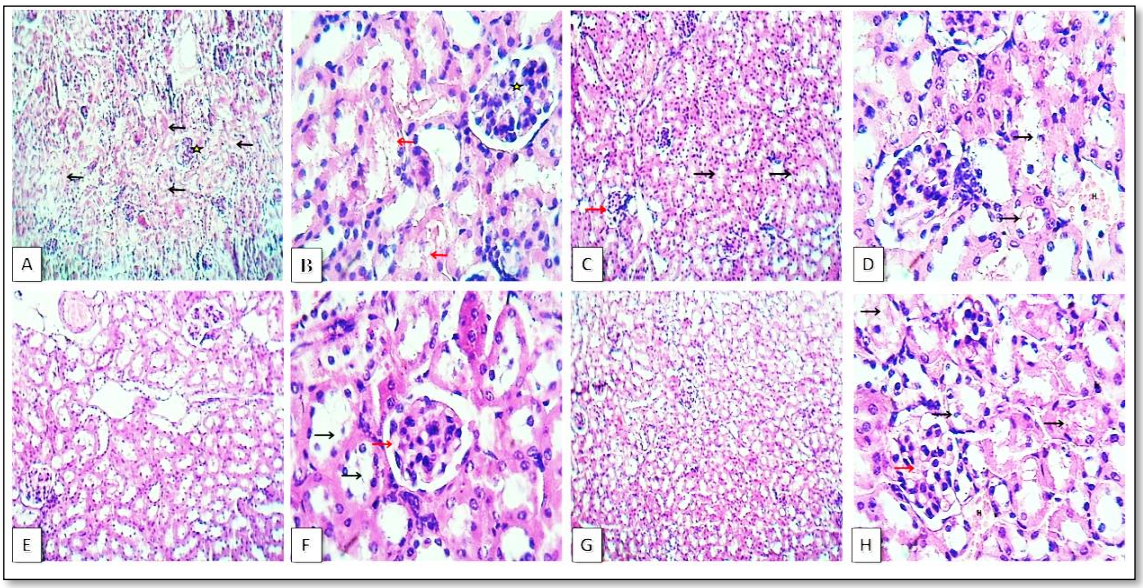

Figure 6. A-H Cross section of renal cortex and medulla in female mice (*Mus musculus*) stained with H&E. 6A-section shows severe nephrosis with marked degeneration & necrosis of lining cells of renal tubules (arrows) with glomerular congestion (asterisks) (H&E, 10x). B-section shows severe nephrosis with marked degeneration & necrosis of lining cells of renal tubules (arrows) with glomerular congestion (asterisks) (H&E, 40x). A C-section shows moderate degeneration of lining cells of renal tubules (black arrows) with glomerular atrophy (red arrow) (H&E, 10x). D-section shows moderate degeneration of lining cells of renal tubules (arrows) with hemorrhage (H) (H&E, 40x). E-section shows mild degeneration of lining cells of renal tubules with glomerular congestion (H&E, 10x). F-section shows mild degeneration of lining cells of renal tubules without necrosis (black arrows) with glomerular congestion (red arrow) (H&E, 40x). G-section shows severe degeneration of lining cells of renal tubules with glomerular congestion (H&E, 10x). The H-section shows severe vacuolar degeneration with necrosis of lining cells of renal tubules (black arrows) with glomerular congestion (red arrow) & hemorrhage (H) (H&E, 40x).

3.5 Histopathological cross sections of MDS-UPEC

Figures 7A-7D show cross-sections of the renal cortex, revealing the normal renal cortex of the control group after staining with H&E. A normal mouse kidney is composed mainly of tubular epithelial cells, convoluted tubules, endothelial cells, podocytes, and mesangial cells, along with Bowman's capsule and Bowman's space. The proximal and distal convoluted tubules appeared normal along with the limning epithelial cells, and there were no signs of vacuolar degeneration, necrosis, or cellular debris within the lumen. The glomeruli appear uniform in architecture, surrounded by Bowman's capsule. Congestion, atrophy, or any damage of podocytes was not seen, and there was hemorrhage, and the blood vessels were normal. The results of the histological sections of the renal cortex of group 2, in which the mice were orally administered ciprofloxacin for a 5-day period after 48 hours of the experiment, showed the appearance of

focal necrosis within renal tubules, mild to moderate in its severity. In addition to the accumulation of mononuclear leukocytes and vascular degeneration with necrosis of lining cells of renal tubules along with the formation of tubular casts, as shown in **Figures 7E** and **7F**. The histological sections of the renal medulla showed mild vascular degeneration of renal tubule lining cells, as shown in **Figure 7G**. As for the renal cortex, vascular degeneration was observed with necrosis of renal tubule lining cells. Clear necrosis around the glomeruli with accumulation of leukocytes, as shown in **Figures 7H** and **8I**. These observations emphasize the nephrotoxic effect of ciprofloxacin, and these findings also highlight the importance of continuously monitoring kidney functions to limit adverse effects of ciprofloxacin on renal health.

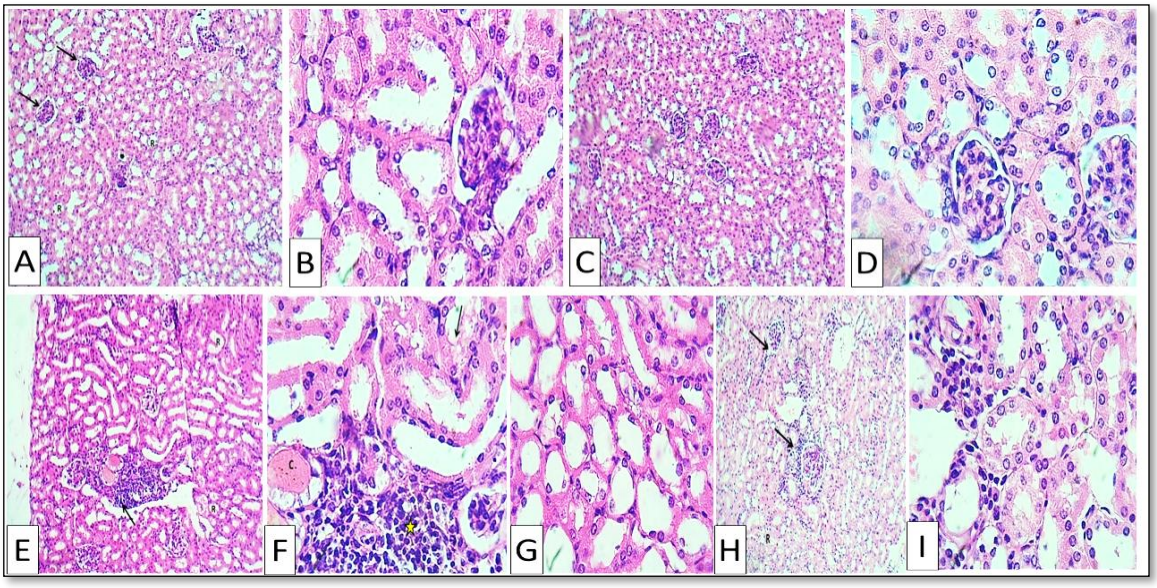

Figure 7. A-I Cross section of renal cortex in female mice (*Mus musculus*) under various conditions stained with H&E. Sections A-D show normal lining cells of renal tubules (R) with normal glomeruli (arrows), A&C sections (H&E, 10x). B&D sections (H&E, 40x). E-section shows focal necrosis of renal tubules (arrow) with vacuolar degeneration of the lining cells of renal tubules (R) (H&E, 10x). F-section shows the renal cortex shows focal necrosis of renal tubules (asterisk) with vacuolar degeneration with necrosis of the lining cells of renal tubules (arrow) and tubular cast formation (C) (H&E, 40x). G-section shows vacuolar degeneration with necrosis of the lining cells of renal tubules (H&E, 40x). H-section shows renal cortex, vacuolar degeneration with necrosis of the lining cells of renal tubules (R) with periglomerular necrosis and aggregation of leukocytes (arrows) (H&E, 10x). The I-section shows vacuolar degeneration with necrosis of the lining cells of renal tubules and aggregation of leukocytes and fibroblasts (H&E, 40x).

Sections presented in **Figures 8A–8D** of group 3 showed severe nephrosis of the renal cortex and medulla after 5 days of oral dosing with ciprofloxacin, characterized by severe degeneration and necrosis of renal tubule lining cells. In addition to observing glomerular degeneration of the mesenteric cells and glomeruli congestion. The histological sections of group 4, orally inducted with the selected isolate (G27), showed simple kidney injury. Vascular degeneration was observed in the renal cortex and medulla with renal tubule lining cell atrophy, in addition to glomeruli atrophy, as shown in **Figures 8E** and **8F**. Interstitial hemorrhage was observed with peri-hemorrhagic cuffing around the mononuclear white blood cells, as shown in **Figures 8G** and **8H**.

As for group 5, the histological sections of renal cortex and medulla had an almost normal appearance compared to group 4. The renal cortex and medulla appeared normal, as did the lining cells of the renal tubules and glomeruli, as shown in **Figure 10A**. Histological sections of some animals belonging to the same group showed moderate vascular degeneration of the cells lining the renal tubules, as shown in **Figures 9B** and **9C**. These differences may be attributed to the level of diversity within animals and to the intensity of the immune system's resistance to infection. Histological sections of group 6 showed vascular degeneration of lining cells of renal

tubules with deterioration of the glomeruli and interstitial edema, as shown in **Figures 9D** and **9E**. Other sections showed severe cellular swelling of the cells lining the renal tubules with severe necrosis, marked deterioration, and glomeruli atrophy, as shown in **Figure 9F**. Considering histological sections of group 7, severe nephrosis with hyperplasia appeared in the lining cells of renal tubules with severe degeneration, interstitial hemorrhage, and formation of tubular casts, as shown in **Figures 10A** and **10B**. Other histological sections showed moderate vascular degeneration of the cells lining the renal tubules with necrosis and tubular dilatation in addition to clear focal necrosis with accumulation of mononuclear WBCs as shown in **Figures 10C** and **10D**.

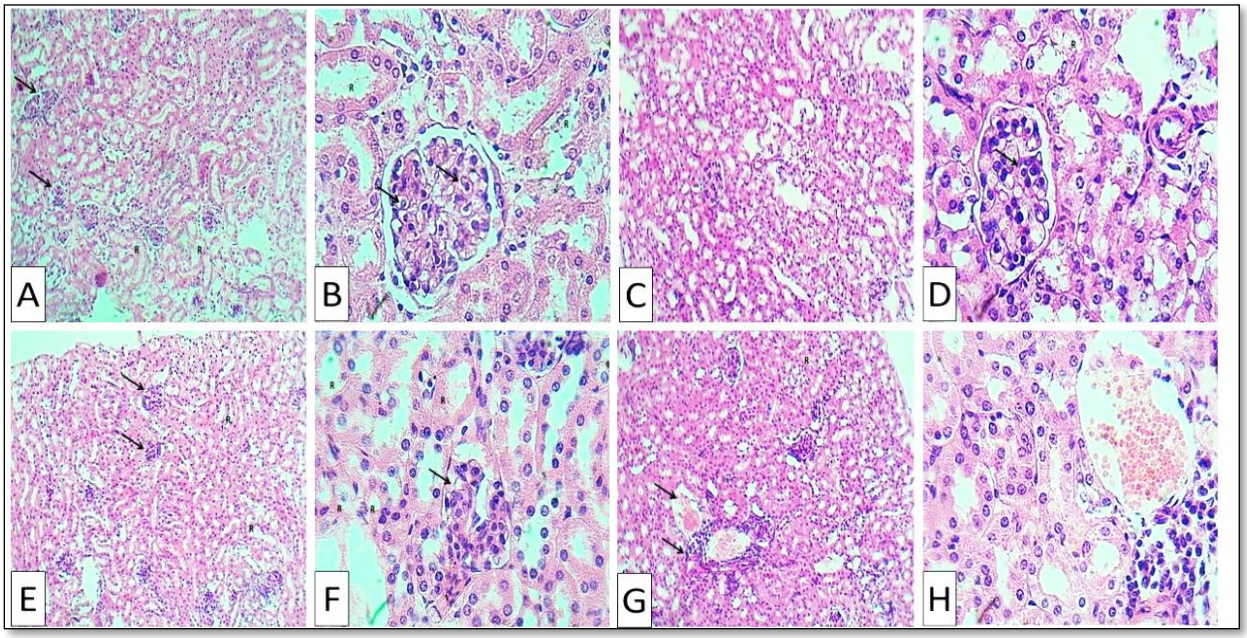

Figure 8. A-H Figure 8A-H shows a cross section of the renal cortex in female mice (Mus musculus) under various conditions, stained with H&E. The A-section shows marked nephrosis characterized by severe degeneration with necrosis of lining cells of renal tubules (R) with glomerular degeneration & congestion (arrows) (H&E, 10x). The B-section shows severe vacuolar degeneration with necrosis of lining cells of renal tubules (R); the glomerulus had degeneration of mesangial cells & congestion (Arrows) (H&E, 10x). The C-section shows marked nephrosis characterized by severe degeneration with necrosis of the lining cells of renal tubules with glomerular degeneration & congestion (H&E, 10x). D-section shows severe vacuolar degeneration with necrosis of lining cells of renal tubules (R) with glomerular congestion (arrow) (H&E, 40x). E-section shows vacuolar degeneration with atrophy of lining cells of renal tubules (R) & glomerular atrophy (arrow) (H&E, 10x). F-section shows vacuolar degeneration with necrosis, atrophy of lining cells of renal tubules (R), & glomerular atrophy (arrow) (H&E, 40x). G-section shows vacuolar degeneration with lining cells of renal tubules (R) & per hemorrhagic cuffing (Arrows) (H&E, 10x). The H-section shows degeneration of lining cells of renal tubules (R) & per hemorrhagic cuffing (H&E, 40x).

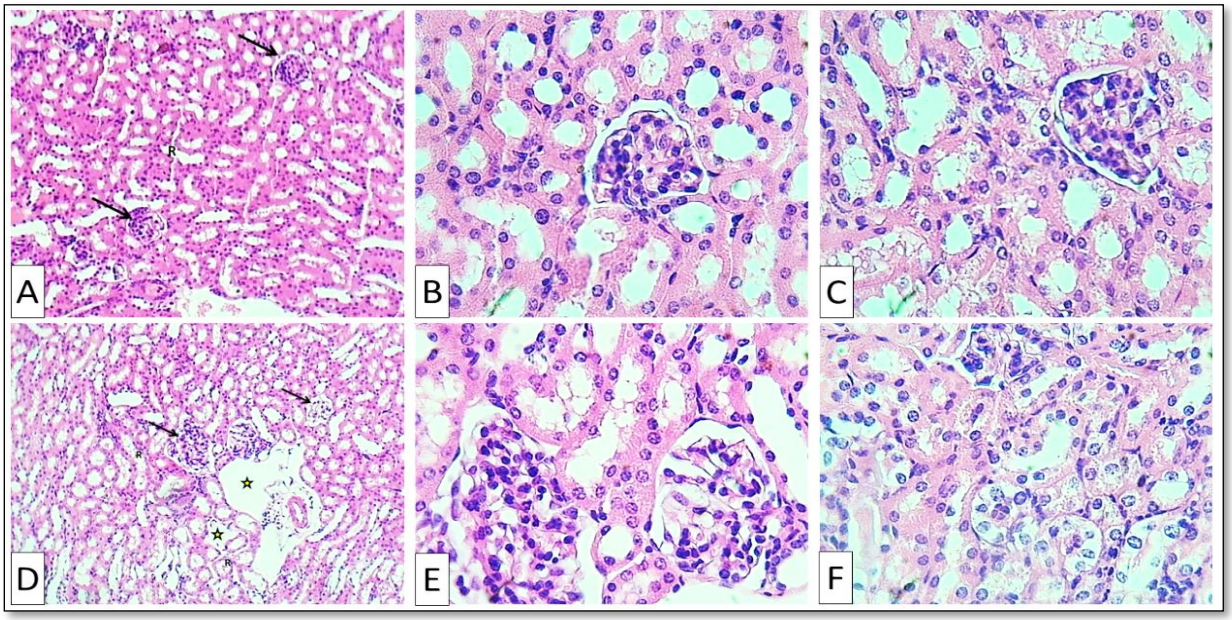

Figure 9. A-F Section of renal cortex in female mice (*Mus musculus*) under various conditions stained with H&E. The A-section shows normal lining cells of renal tubules (R) & glomeruli (arrows) (H&E, 10x). The B-section shows normal lining cells of renal tubules & normal glomerulus (H&E, 40x). A C-section shows moderate vacuolar degeneration of the lining cells of renal tubules with necrosis (H&E, 40x). D-section shows vacuolar degeneration of lining cells of renal tubules (R) & deterioration of glomeruli (arrows) & interstitial edema (asterisks) (H&E, 10x). E-section shows vacuolar degeneration of lining cells of renal tubules without necrosis & deterioration of glomeruli (H&E, 40x). F-section shows vacuolar degeneration & cellular swelling of lining cells of renal tubules with necrosis & deterioration of glomeruli (H&E, 40x).

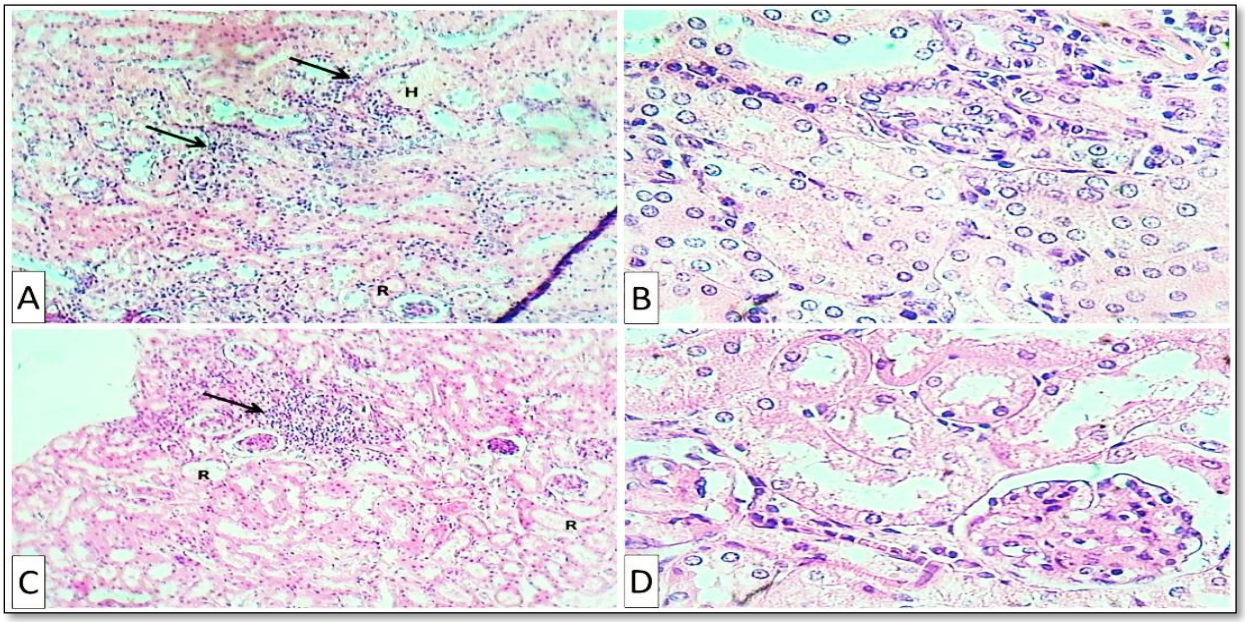

Figure 10. A-D The figure displays a section of the renal cortex in female mice (Mus musculus) under various conditions, which has been stained with Hematoxylin and Eosin (H&E). A-section shows nephrosis with hypercellularity of lining cells of renal tubules & hemorrhage (H) & cast formation (R) (H&E, 10x). The B-section shows hyperplasia of lining cells of renal tubules & degeneration (H&E, 40x). C-section shows vacuolar degeneration of lining cells of renal tubules with necrosis and tubular dilation (R) & focal necrosis with aggregation of mononuclear leukocytes (Arrow) (H&E, 10x). D-section shows vacuolar degeneration of lining cells of renal tubules with necrosis (H&E, 40x).

4. Discussion

The finding highlights that these doses were ineffective to establish infection under the tested conditions. These results align with [15], which reported that the sub-threshold bacterial loads fail to initiate infections due to host ability to clear and neutralize small doses of invading bacteria. The insufficient loads may not trigger a defense mechanism against the host immune response, such as the quorum sensing system, which eventually increases the pathogenicity by leading to biofilm formation. These observations highlight the importance of bacterial concentration to induce sufficient infection in animal modules. These outcomes indicate that high doses of bacterial loads induce systematic toxicity, sepsis, organ failure, and death [15].

Several studies investigate and document the required bacterial load to induce UTI infections and the outcomes of them on body systems. As vouch by [16] that 10^7cell/ml load was sufficient to induce infection across many organs, such as the liver, spleen, brain, lungs, and kidneys. According to [16], the infection rapidly disseminated with the presence of bacterial cells within organs after 20 minutes, peaking after 24 hours post-infection, and there were no mortalities among the animals, which means that this load was able to induce a systematic infection without causing fatal outcomes. In addition [17] corroborated the findings of [16], highlighting the potential activity of a bacterial load of 10^7 cells/ml to induce UTI infection. In contrast, according to [21], even the low bacterial load of 10^5 cells/ml was capable of causing UTIs. Also [22] noted that the bacterial load decreased overtime in most organs, but they remained persistent in tissues for 48 hours. [18] extend the research for the bacterial loads and their impacts on establishing infection using animal models. The bacterial load of 10^8 cells/ml was used to establish primary and secondary infections within 1-6 hours. It is interesting that even at high doses (10^8 cells/ml), no mortalities were recorded, and it significantly increased the bacterial loads and inflammatory responses. These observations highlight the critical role of secondary infection in inducing the infection. The bacterial presence nature, which decreases after 24 hours, highlights the importance of the timeline of bacterial proliferation and host immune response, which was conducted by the elevation of IL-6, CXCL1, and G-CSF after the secondary infection, which means the severity of infection. [19] revealed the impact of high bacterial load (10^9 cells/ml), which causes significant physiological and pathological changes. It was noted that mice inducted with high bacterial loads exhibited weight reduction and 20% mortality rates due to the severity of infection, which was linked to the acidic environment that enhances *E. coli* virulence. These findings suggest the relationship between high bacterial load and host tissue damage leads to weight loss and mortalities.

Fluoroquinolones such as ciprofloxacin are known for their widespread use in healing bacterial infections, although they have exhibited their toxicity at high doses on the central nervous system, digestive system, and kidney. Over 200mg/kg, doses have been reported for their significant organ damage and mortalities in animal models. [20] reported that high doses could disrupt oxidative stress and lead to kidney failure, which would make the kidney lose its function. These findings highlight the interference of high ciprofloxacin doses with mitochondrial function and activity, which leads to increased oxidative stress and dysfunction of cells and ultimately leads to organ failure. These results emphasize that ciprofloxacin could be potentially toxic after administration in high amounts, and this highlights the importance of dose regulation. In addition to its toxic effect on both kidneys and the digestive system, it also exhibits neurological toxicity at high concentrations. Behavioral changes of animals have also been documented due to high concentrations of ciprofloxacin. [21] established 20 and 50 mg/kg on mice with a 14-day period and reported that ciprofloxacin significantly resulted in behavioral changes in animals with highly reduced locomotor activity. These findings suggest that the neural function altered due to ciprofloxacin, which came as a result of affecting the oxidative stress pathway. Furthermore, [22] investigated the effect of ciprofloxacin on memory and cognition and demonstrated that ciprofloxacin can impair the memory function of mice. These results align with the hypothesis that ciprofloxacin can successfully affect oxidative stress by disrupting the

balance of neurotransmitters, which finally affects behavior and cognitive performance, but it is still not fatal, but it may increase the incidence of mortalities in the future. Ciprofloxacin impact on body weight, behavioral responses, and some hematological parameters in experimental animals highlighted by [23] and indicated that body weight was not significantly affected by ciprofloxacin no matter the dose or duration of it. This is attributed to antioxidants such as vitamins A, C, and E, which maintain the physiological balance and prevent volatility of body weight. Also, they noticed that ciprofloxacin could alter red blood cell amount, especially when it is administered at high doses, and eventually lead to fatigue and lethargy. Also, [24] report the effect of ciprofloxacin for a short period of administration and conclude that ciprofloxacin had no effect on body weight, while [25] demonstrate that ciprofloxacin can significantly increase body weight after exposure to high doses and for a long period. These findings are attributed to the impact of ciprofloxacin on gut microbiota, which are responsible for metabolism and different nutrient absorption, so any disturbance in the microbiota, such as ciprofloxacin, can increase nutrient assimilation, which leads to weight gain. Similarly, [26] report the impact of long-term ciprofloxacin administration may lead to mortalities in animal modules by affecting gut microbiota, which compromises the animal immune system.

Ciprofloxacin is known for its nephrotoxic effect; according to [27], ciprofloxacin could cause significant cellular changes represented by glomeruli alterations. These alternations include inflammation, tubular necrosis, congestion, and obstruction of renal tubules. In addition, the interstitial space exhibits fibrosis, which refers to chronic damage. All of these observations result from ciprofloxacin, which induces oxidative stress and nephrotoxic effects. Also, [28] demonstrate ciprofloxacin impact on kidney injury and how it could be reduced using quercetin. It was reported that prolonged exposure to ciprofloxacin leads to kidney injury characterized by tubular necrosis, glomeruli congestion, and inflammation of the interstitial space, which are considered oxidative stress markers. Ciprofloxacin is known for its nephrotoxicity, especially on the renal cortex, and leads to many histological alterations, such as necrosis and glomeruli congestion [29, 30].

The study of [31] highlighted the impact of *E. coli* infection, which results in many inflammatory responses and tissue damage. They noticed peaked levels of pro-inflammatory cytokines such as IL-6, IL-1β, and TNF-α, especially after the seven-day post-infection period; these cytokines reflect the body response to eliminate bacterial invasion. The bacterial infection also led to the induction of oxidative stress characterized by an increase of nitric oxide synthase, which causes tissue injury. *E. coli infections* also cause notable damage, such as mitochondrial swelling with atrophy along with secondary lysosomes and autophagolysosomal bodies. According to [32], the histopathological changes of *E. coli* infection are marked with severe swelling of renal epithelial cells and reduction in size of tubular lumen size; these observations lead to impairment of tubular function. Also, widespread necrosis was observed in renal tissue, indicating cell death due to bacterial toxins. In addition, hemorrhage within the renal cortex was observed, which causes loss of vascular integrity and bleeding. Nevertheless, all of these observations came in line with some blood markers: elevated neutrophils and reduced thrombocyte levels. In another study, [33] demonstrate the histopathological changes in the kidney due to *E. coli* infection. Acute Tubular necrosis was observed again along with degeneration of lining epithelial cells of renal tubules. Also, glomeruli were abnormal and contained fibrin clots within blood capillaries, and hemorrhage was observed due to red blood cell accumulation. These observations suggest unsuccessful filtration with vascular damage.

5. Conclusion

The results of the current study provide important insights on the efficacy and nephrotoxic effect of ciprofloxacin as a treatment for MDR-UPEC and MDS-UPEC. The infection of MDR-UPEC reflects more damage than MDS-UPEC. Ciprofloxacin demonstrates high antibacterial activity against bacterial load in murine models, notably by the disappearance of the bacterial

toxicity with renal tissue after inducting it with MDR-UPEC, while MDS-UPEC showed less aggressive damage to the renal tissue. However, its nephrotoxicity was evident, such as necrosis, degeneration, and atrophy of glomeruli.

Acknowledgment

We thank the Iraqi Center for Cancer Research and Medical Genetics, Al-Mustansiriya University, Baghdad, Iraq, for facilitating the practical part of this article.

Conflict of Interest

Estabraq A. Mahmoud declares that she is a member of IHJPAS editorial board at the time of submitting the manuscript. The editor-in-chief of IHJPAS confirms that (Estabraq A. Mahmoud) was excluded from any decisions made regarding this article.

Funding

No funding.

Ethical Clearance

All animals were approved by the Iraqi Center for Cancer Research and Medical Genetics ethical committee (Numb. 2353 at 23/10/2024) in accordance with institutional guidelines for the care and use of laboratory animals.

References

1. Mlugu EM, Mohamedi JA, Sangeda RZ, Mwambete KD. Prevalence of urinary tract infection and antimicrobial resistance patterns of uropathogens with biofilm forming capacity among outpatients in Morogoro, Tanzania: a cross-sectional study. BMC Infect Dis. 2023;23(1):660. https://doi.org/10.1186/s12879-023-08641-x
2. Shah C, Baral R, Bartaula B, Shrestha LB. Virulence factors of uropathogenic Escherichia coli (UPEC) and correlation with antimicrobial resistance. BMC Microbiol. 2019;19:204. https://doi.org/10.1186/s12866-019-1587-3.
3. Raoof MAJ, Fayidh MA. Molecular study to detect blaTEM and blaCTX-M genes in ESβL Escherichia coli and their antimicrobial resistance profile. J Phys Conf Ser. 2021;1879(2):022051. https://doi.org/10.1088/1742-6596/1879/2/022051
4. Hamady DR, Ibrahim SK. The study on ability of Escherichia coli isolated from different clinical cases to biofilm formation and detection of csgD gene responsible for produce Curli (Fimbriae). Biochem Cell Arch. 2020;20(2):[page numbers not specified].
5. Al-Zaidi,O.S.S.H, Zwain, L.A. and Mahmoud, E.A. Effect of ciprofloxacin and Trimethoprim/Sulfamethoxazole on Biofilm formation of Multi-Drug Resistant Uropathogenic Escherichia coli. Int. J. Des. Nat. Ecodyn. 2025; 20(4):691-703. http://doi:10.18280/ijdne.200401.
6. Raoof MAJ, Fayidh MA. Investigation of biofilm formation efficiency in ESβLs of pathogenic Escherichia coli isolates. Int J Drug Deliv Technol. 2022;12(2):695–700.
7. Bunduki GK, Heinz E, Phiri VS, Noah P, Feasey N, Musaya J. Virulence factors and antimicrobial resistance of uropathogenic Escherichia coli (UPEC) isolated from urinary tract infections: a systematic review and meta-analysis. BMC Infect Dis. 2021;21:1–13. https://doi.org/10.1186/s12879-021-06435-7
8. Bryce A, Hay AD, Lane IF, Thornton HV, Wootton M, Costelloe C. Global prevalence of antibiotic resistance in paediatric urinary tract infections caused by Escherichia coli and association with routine use of antibiotics in primary care: systematic review and meta-analysis. BMJ. 2016;352:i939. https://doi.org/10.1136/bmj.i939
9. Chockalingam A, Stewart S, Xu L, Gandhi A, Matta MK, Patel V, Sacks L, Rouse R. Evaluation of immunocompetent urinary tract infected Balb/C mouse model for the study of antibiotic resistance development using *Escherichia coli* CFT073 infection. Antibiotics. 2019;8:170. https://doi.org/10.3390/antibiotics8040170

10. Campbell RE, Chen CH, Edelstein CL. Overview of antibiotic-induced nephrotoxicity. Kidney Int Rep. 2023;8:2211–2225.
11. Crellin E, Mansfield KE, Leyrat C, Nitsch D, Douglas IJ, Root A, Williamson E, Smeeth L, Tomlinson LA. Trimethoprim use for urinary tract infection and risk of adverse outcomes in older patients: cohort study. BMJ. 2018;360:k341. https://doi.org/10.1136/bmj.k341
12. Tille PM. Baily and Scott's Diagnostic Microbiology. 12th ed. St. Louis: Mosby, Inc., Elsevier; 2021.
13. Nair AB, Jacob S. A simple practice guide for dose conversion between animals and human. J Basic Clin Pharm. 2016;7(2):27–31. https://doi.org/10.4103/0976-0105.177703.
14. Bancroft JD, Layton C. The hematoxylins and eosin. In: Bancroft JD, Layton C, editors. Bancroft's Theory and Practice of Histological Techniques. 7th ed. Shanghai: Churchill Livingstone Elsevier Ltd.; 2013. p. 173–86.
15. Hannan TJ, Mysorekar IU, Hung CS, Isaacson-Schmid ML, Hultgren SJ. Early severe inflammatory responses to uropathogenic E. coli predispose to chronic and recurrent urinary tract infection. PLoS Pathog. 2010;6(8):e1001042. https://doi.org/10.1371/journal.ppat.1001042
16. Smith SN, Hagan EC, Lane MC, Mobley HL. Dissemination and systemic colonization of uropathogenic Escherichia coli in a murine model of bacteremia. mBio. 2010;1(5):e00262-10. https://doi.org/10.1128/mBio.00262-10.
17. Narayanan A, Muyyarikkandy MS, Mooyottu S, Venkitanarayanan K, Amalaradjou MA. Oral supplementation of trans-cinnamaldehyde reduces uropathogenic Escherichia coli colonization in a mouse model. Lett Appl Microbiol. 2017;64(3):192–7. https://doi.org/10.1111/lam.12713.
18. Schwartz DJ, Chen SL, Hultgren SJ, Seed PC. Population dynamics and niche distribution of uropathogenic Escherichia coli during acute and chronic urinary tract infection. Infect Immun. 2011;79(10):4250–9. https://doi.org/10.1128/IAI.05339-11.
19. Herrera-Espejo S, Domínguez-Miranda JL, Rodríguez-Mogollo JI, Pachón J, Cordero E, Pachón-Ibáñez ME. Effects of pH on the pathogenicity of Escherichia coli and Klebsiella pneumoniae on the kidney: *In vitro* and *in vivo* studies. Int J Mol Sci. 2024;25(14):7925. https://doi.org/10.3390/ijms25147925.
20. Weyers AI, Ugnia LI, Ovando HG, Gorla NB. Ciprofloxacin increases hepatic and renal lipid hydroperoxides levels in mice. Biocell. 2002;26(2):225–8.
21. Ilgin S, Can OD, Atli O, Ucel UI, Sener E, Guven I. Ciprofloxacin-induced neurotoxicity: evaluation of possible underlying mechanisms. Toxicol Mech Methods. 2015;25(5):374–81. https://doi.org/10.3109/15376516.2015.1026008.
22. Alhowail AH. Ciprofloxacin produces memory deficits in male mice. Int J Pharmacol. 2020;16(1):27–32. https://doi.org/10.3923/ijp.2020.27.32.
23. Priyadharshini KM. Ciprofloxacin induced body weight and haematological changes in rats and antioxidant vitamin A, C and E as rescue agents. Int J Eng Sci Invention. 2013;22:21–31. https://doi.org/10.9790/3008-0531218.
24. Norville IH, Hatch GJ, Bewley KR, Atkinson DJ, Hamblin KA, Blanchard JD, Armstrong SJ, Pitman JK, Rayner E, Hall G, Vipond J, Atkins TP. Efficacy of liposome-encapsulated ciprofloxacin in a murine model of Q fever. Antimicrob Agents Chemother. 2014;58(9):5510–5518. https://doi.org/10.1128/AAC.03443-14
25. Islam MS, Belal B, Dash S, Islam MS, Hasan MM. Chronic exposure of ciprofloxacin antibiotic residue above the MRL level and its pathophysiological effects in mice. Curr Res Complement Altern Med. 2024;8(249):2577–2201. https://doi.org/10.29011/2577-2201.100249.
26. Zarrinpar A, Chaix A, Xu ZZ, Chang MW, Marotz CA, Saghatelian A, Knight R, Panda S. Antibiotic-induced microbiome depletion alters metabolic homeostasis by affecting gut signaling and colonic metabolism. Nat Commun. 2018;9:2872. https://doi.org/10.1038/s41467-018-05336-9.
27. Al-Shawi NN. Possible histological changes induced by therapeutic doses of ciprofloxacin in liver and kidney of juvenile rats. Pharmacologia. 2012;3(9):477-480. https://doi.org/10.5567/pharmacologia.2012.477.480.
28. Elbe H, Dogan Z, Taslidere E, Çetin A, Turkoz Y. Beneficial effects of quercetin on renal injury and oxidative stress caused by ciprofloxacin in rats: A histological and biochemical study. Hum Exp Toxicol. 2016;35(3):276-281. https://doi.org/10.1177/0960327115584686 SAGE Journals

29. Khudhiar AS, Al-Khamas AJ, Hadi SJ, Murad MM, Faris JK, Zballa Almermdhy HAE. Effect of hesperidin and ciprofloxacin on the function and histological structure of kidney in local male rabbits. Biochem Cell Arch. 2019;19(2):4279-4283.
30. Genid AAK, Ibrahim A, Elagwany AM, Yehia MAH, Biram DM. The Effect of Ciprofloxacin on Renal Cortex of Adult Male Albino Rat and the Possible Protective Role of Olive Oil: Anatomical and Histological Study. Egypt J Histol. 2023;46(3):1494-1511. https://doi.org/10.21608/ejh.2022.143262.1701 Egyptian Journal of Histology
31. Long N, Deng J, Qiu M, Zhang Y, Wang Y, Guo W, Dai M, Lin L. Inflammatory and pathological changes in Escherichia coli infected mice. Heliyon. 2022;8(12):e12533. https://doi.org/10.1016/j.heliyon.2022.e12533
32. Al-Zamely H, Falh S. The Effect of Experimental Escherichia coli Infection on Some Blood Parameters and Histological Changes in Male Rats. Iraqi J Vet Med. 2011;35(2):22-27. https://doi.org/10.30539/iraqijvm.v35i2.571 jcovm.uobaghdad.edu.iq
33. Eaton KA, Friedman DI, Francis GJ, Tyler JS, Young VB, Haeger J, Abu-Ali G, Whittam TS. Pathogenesis of renal disease due to enterohemorrhagic Escherichia coli in germ-free mice. Infect Immun. 2008;76(7):3054-3063. https://doi.org/10.1128/IAI.01626-07